UNIVERSIDAD SAN FRANCISCO DE QUITO USFQ

Colegio de Ciencias e Ingenierías

SYNTHESIS OF ADVANCED Co$_3$O$_4$/BiFeO$_3$ COMPOSITE MATERIALS, AND THEIR APPLICATION IN THE DEGRADATION OF ORGANIC DYES

José Roberto Daza Acosta

Ingeniería Ambiental

**Trabajo de integración curricular presentado como requisito
para la obtención del título de
Ingeniero Ambiental**

Quito, 17 de diciembre de 2019

UNIVERSIDAD SAN FRANCISCO DE QUITO USFQ

Colegio de Ciencias e Ingenierías

HOJA DE CALIFICACIÓN
DE TRABAJO DE INTEGRACIÓN CURRICULAR

SYNTHESIS OF ADVANCED Co$_3$O$_4$/BiFeO$_3$ COMPOSITE MATERIALS, AND THEIR APPLICATION IN THE DEGRADATION OF ORGANIC DYES

José Roberto Daza Acosta

Calificación:

Nombre del profesor, Título académico   Thomas Cadenbach, Dr. rer. nat.

Firma del profesor: _____

Quito, 17 de diciembre de 2019

Derechos de Autor

Por medio del presente documento certifico que he leído todas las Políticas y Manuales de la Universidad San Francisco de Quito USFQ, incluyendo la Política de Propiedad Intelectual USFQ, y estoy de acuerdo con su contenido, por lo que los derechos de propiedad intelectual del presente trabajo quedan sujetos a lo dispuesto en esas Políticas.

Asimismo, autorizo a la USFQ para que realice la digitalización y publicación de este trabajo en el repositorio virtual, de conformidad a lo dispuesto en el Art. 144 de la Ley Orgánica de Educación Superior.

Firma del estudiante:
-------------------------_____

Nombres y apellidos: José Roberto Daza Acosta

Código: 00106509

Cédula de identidad: 1717609182

Lugar y fecha: Quito, 17 de diciembre de 2019

AGRADECIMIENTOS

RESUMEN

La Rodamina B (RhB), es un colorante orgánico de uso intensivo en la industria textil. Este representa un amenaza considerable al medio ambiente ya que muchas veces es desechado directamente en cuerpos de agua sin una gestión o tratamiento adecuado. La Agencia de Protección del Medio Ambiente de los Estados Unidos (EPA por sus siglas en inglés), lo clasifica y describe dentro de registros como la base de datos de sustancias peligrosas, la base de datos de ecotoxicología y el inventario de manejo de sustancias tóxicas. (EPA,2019). Debido a su alta estabilidad, poca biodegradabilidad y toxicidad se recurre a procesos de oxidación avanzada para la degradación y remoción de este contaminante de un sistema acuoso. Los compuestos Co_3O_4, y $BiFeO_3$ son conocidos y estudiados por su capacidad de actuar como fotocatalizadores en los procesos de fotocatálisis para la degradación de colorantes orgánicos. En el presente estudio se sintetizaron nanopartículas porosas de Co_3O_4, y $BiFeO_3$, posteriormente se caracterizaron dichas nanopartículas de Co_3O_4 y $BiFeO_3$ por medio de análisis de difracción de rayos X (XRD) y microscopía de transmisión de electrones (TEM). Los compuestos obtenidos fueron sometidos a procesos fotocatalíticos para evaluar su capacidad de degradación del colorante RhB. Los resultados indicaron una mejor capacidad de adsorción del compuesto Co_3O_4 debido a su naturaleza porosa, lo que dio en general un mejor rango de remoción de RhB de una muestra de agua. Esta capacidad fue mejorada significativamente con la adición de un agente quelante llamado ácido nitriloacético (NTAA). El mismo que fue utilizado para la formación de un material compuesto de $Co_3O_4/BiFeO_3$ el cual produjo prometedores resultados en la adsorción/degradación de la Rodamina B de una muestra de agua.

Palabras clave: Co_3O_4, nanoporoso, $BiFeO_3$, nanocompuesto, adsorción, fotocatálisis, rodamina B, agente quelante, colorantes, contaminación industrial.

ABSTRACT

Rhodamine B (RhB) is an example of a highly used organic dye in the textile industry. This contaminant represent a hazardous waste that could highly damage the environment. Evidence have shown that these type of wastes have been realized directly to water bodies without a proper management or treatment of any kind. The U.S. Environmental Protection Agency (EPA), describes and includes this contaminant in the EPA hazardous substances data bank, EPA ecotoxicology knowledgebase, and the EPA toxics release inventory, just to mention a few examples (EPA, 2019). Thanks to its high stability, poor biodegradability, and toxicity, advanced oxidation process (AOPs) have to be used for the removal and degradation of this contaminant from an aqueous system. Catalysts Co_3O_4, and $BiFeO_3$ are known and studied for their capacity to act as a photocatalyst in a photocatalysis process. In the present study porous nanoparticles of Co_3O_4, and $BiFeO_3$ were synthesized. Subsequently characterization analysis were carried out by using X ray diffraction (XRD), and transmission electron microscopy (TEM). The obtained compounds were used in a photocatalytic process in order to evaluate their RhB degradation capability. Results shown a better adsorption capacity from Co_3O_4 thanks to its porous composition, which produced a better remotion capacity of RhB. This capacity was enhanced by the addition of a chelating agent called nitrilo acetic acid (NTAA). This chelating agent which has the ability to produce coordination complexes, was used in the formation of a $Co_3O_4/BiFeO_3$ nanocomposite material that produced promising results in the adsorption/degradation of RhB from a water sample.

Key Words: Co_3O_4, nanoporous, $BiFeO_3$, nanocomposite, adsorption, photocatalysis, rhodamine B, chelating agent, dye, industrial contamination.

CONTENT TABLE

List of Figures

1. **Introduction**

    'Water quantity challenges receive a great deal of attention from the development community, but water quality impacts may be equally, or more, important' (Damania, R. et al, 2019). The world experimented many transformations thanks to the great industrial revolution. A rapid economic expansion, the appearance of new technologies, and the development of many industries, among the most important transformations (Damania, R. et al, 2019). Furthermore, there's been a close relationship between water quality and the industrial development. Economists Gene Grossman and Alan Krueger concluded that water pollution would describe a inverted-U pattern with respect to economic and industrial development; In other words, as economies grow and develop, pollution will increase (Grossman, G. Krueger, a. 1995).

    The world bank mentions that, in developing countries more than 90 percent of waste water is still discharged into water bodies without any treatment (Damania, R. et al, 2019). The fact that water quality remains a big issue, despite the long research and knowledge about the impacts of industrial discharges in water quality, it's proof of the high complexity of industrial water pollution around the world (Damania, R. et al, 2019).

    In particular, there must be special attention to the textile industry. According to the National Council of Textile Organizations in the U.S.A. (NCTO), this sector represented over $75 billion in shipments in 2017 (NCTO, 2017). Moreover, textile industry also represents an important source of contaminated effluents due to the large quantities of water used in the dyeing process (Pereira, L. Alves, M. 2014). In addition, the textile sector consumes close to ⅔ rds of the entire synthetic dye production, which makes this industry the largest consumer of synthetic dyes in the world (Pereira, L. Alves, M. 2014).

    Dye contaminated water presents an important challenge due to the toxic compounds such as xanthene, benzene, aromatic amines, and many other hazardous components that

organic heterocyclic dyes possess (Sharifzade, G. et al, 2017). Rhodamine B is a cationic xanthene dye, that has proven to be an efficient fluorescent dye, and that has many industrial applications. It's frequently used in the textile industry, and can be found in the wastewater produced after some dyeing processes. Furthermore, Rhodamine B presence in wastewater represent a serious environmental issue due to its toxicity and stability in the environmental matrix (Sharifzade, G. et al, 2017).

Advanced oxidation processes (AOPs) present a cost effective and efficient alternative to mineralize and degrade stable, and toxic dyes such as Rhodamine B (Hodges, B. et al, 2017). Photocatalysis is a light driven AOP in which nano semiconductor particles get excited in the presence of light photons, which triggers valence band (VB) spaces, and conduction band (CB) electrons (e-), unleashing a group a redox reactions at the catalyst surface (Hodges, B. et al, 2017). This process that according to the literature is been developed for many years, have been focussing mostly in the applications of TiO_2 as a catalyst for AOPs. However, there are also important contributions to the development, and research of newer and more efficient photocatalysts, with the ability to get excited in the presence of visible light (>420 nm) (Hodges, B. et al, 2017). Two materials that are receiving a great deal of attention for their good photocatalytic characteristics are cobalt oxide Co_3O_4 and single-phase bismuth ferrite $BiFeO_3$ (Cadenbach, T. et al, 2019). On the one side, Co_3O_4 is the most stable cobalt oxide, and because of that is been used for several technological applications such as water splitting, contaminant removal and battery cathodes (Saeed, M. et al, 2018). Co_3O_4 can be synthesized using different synthetic methods, but the most important thing is that achieving a well defined morphology (Edla, R. et al, 2014), high porosity, and narrow band gap is crucial in order to benefit from this compound's adsorbent and catalytic characteristics (Hassanpour, M. et al, 2017).

On the other side, even though the achievement of a pure single-phase $BiFeO_3$ is very complex (Cadenbach, T. et al, 2019), these nanoparticles have demonstrate to have a great photocatalytic capacity due to their relative narrow band gap ($\sim$2.1–2.8 eV) (Cadenbach, T. et al, 2019). Moreover, literature have shown that BFO nanoparticles are responsible for the water splitting, and degradation of organic dyes such as Rhodamine B (Lam, S. et al, 2017). Additionally the creation of nanocomposites enforces the photocatalytic capabilities that a single semiconductor could have. (Chen, G. et al, 2015)

In this study we first report a facile synthesis method for Co_3O_4 and $BiFeO_3$ respectivetely, using nanocasting and sol-gel methods to create an advanced Co_3O_4 / $BiFeO_3$ nanocomposite material that could enhance photocatalytic degradation of RhB. Resulting product was characterized using X ray diffraction (XRD), and transmission electron microscopy (TEM). Posteriorly, the nanocomposite material was used in the photocatalytic degradation of a solution of Rhodamine B (50 mg/L) in a visible light LED reactor (λ>420 nm), which produced promising results of dye adsorption/degradation.

2. Experimental details

2.1 Materials and methods

All the reagents used in this study were purchased from Sigma Aldrich analytical level without further purification. Synthetic conditions were maintained at room temperature for all synthesis which are favorable conditions reported in the literature (Binitha, P. et al, 2010). X Ray diffraction patterns were recorded by a Bruker Phaser D2 in a 2θ configuration. Transmission electron microscopy (TEM) images were produced by a FEI Tecnai G2 spirit twin, with accelerating voltage of 20-120 kV / LaB_6.

2.2 Synthesis of Co₃O₄ nanoparticles

Co_3O_4 nanoparticles were synthesized by follow the 2 step impregnation method reported in (Deng, X. et al, 2018) . In a typical experiment, with a 24% impregnation rate, a 8 molar solution of $Co(NO_3)_2$. 6 H_2O and ethanol was produced under vigorous stirring after 1 hour approximately. Around 50 % of that solution was separated for later use, and the remaining solution was mixed with SBA-15 or KIT-6, depending on desired morpho structure (Deng, X. et al, 2018). After two hour of stirring at room temperature, solution was dried overnight at 80 °C. A bright pink powder was obtained, and calcined afterwards at 450 °C for 6 hours.

After the calcination process the first separated solution was added back for the second impregnation and was left at vigorous stirring for 2 hours. Finally the sample was dried overnight at 80 °C. Final product was a black powder.

2.3 Synthesis of BiFeO₃ precursor nanoparticles

For the synthesis of BFO nanoparticles a one-step wet impregnation process was performed (Gao, T. et al, 2015). Calculated stoichiometric amount of $Bi(NO_3)_3$. 5 H_2O, $Fe(NO_3)_3$. 9H_2O, and $C_4H_6O_6$ (Tartaric acid), were mixed together in a 2-Methoxyethanol solution. Drops of a solution 2 M of HNO_3 were added to favor the mixture. This BFO complex was dried and concentrated in a rotavapor equipment, in which solvent was recovered. Finally the sample was dried in the oven overnight at 60 °C. The resulting product was a dark yellow powder.

2.4 Preparation of Co₃O₄ - BiFeO₃ nanocomposite

For the comparison and evaluation of the photocatalytic capability, three experiments were performed. First, a sol-gel method was used to synthesize the composite material. $BiFeO_3$

and Co_3O_4 were added to a 2-Methoxyethanol solution and left under vigorous stirring for 2 hours, drops of a 2M HNO_3 solution were added to favor the mixture of the components. After the 2 hours of stirring the solution was concentrated and dried in a rotavapor equipment. Resulting powder after the drying process was added directly to a 50 mg/L solution of Rhodamine B in order to evaluate its photocatalytic activity.

Second, $BiFeO_3$ and Co_3O_4 were added directly to the Rhodamine b solution, with the extra addition of a Nitriloacetic acid (NTAA), which is a chelating agent. Finally, same method was applied for the addition of ethylenediaminetetraacetic acid (EDTA), another chelating agent. Followed to this processes, photocatalytic degradation of Rhodamine B, was evaluated.

2.5 Photo-catalytic evaluation

The photocatalytic degradation efficiency, and adsorption removal was evaluated for organic dye Rhodamine B, and was recorded by a GENESYS 30 Visible spectrophotometer. For a typical experiment, a 50 mg/L solution of Rhodamine B was prepared using distilled water. Individual photocatalyst and composite photocatalysts were evaluated using this solution, and a high power LED reactor with an emission wavelength > 420 nm. Synthetic conditions such as room, and reactor temperature was controlled, and the experiment was performed under vigorous stirring. For every experiment, solution with photocatalyst was stirred in the absence of light for a 1 hour period. Literature mentions that this time is necessary in order to reach an adsorption / desorption equilibrium (Cadenbach, T. et al, 2019). After 1 hour in the darkness, absorbance was measured every 30 min, for a period of 4 hours in total. Maximum peaks of UV-vis absorbance spectra were measured taking into account that concentration can be determine by the Beer-Lambert equation, which makes a correlation between intensity of absorbance and molecules concentration. Absorbance was converted to concentration by using a Rhodamine B calibration curve previously prepared.

3. Results and Discussion

3.1 Characterization

In the previous section a synthesis method was described as the method that was used to obtain Co_3O_4 and $BiFeO_3$ in a pure phase. X Ray diffraction analysis (XRD), were carried out to evaluate the presence of the crystalline phase of the compounds used in the synthesis of a composite material. Fig. 1 shows an X ray diffractogram of prepared catalyst Co_3O_4. The different peaks present in this graphic indicate that crystallinity nature of the compound. Therefore, Peaks at $2\theta = 19.043°$, $31.341°$, $36.878°$, $44.675°$, and $59.180°$ are assigned to (1 1 1), (2 2 0), (3 1 1), (2 2 2), (4 0 0) and (5 1 1) lattices of Co3O4 respectively, as reported by (Saeed, M. et al, 2017) . Moreover, similar results were also reported by other researchers such as (Mashayekhi, M. et al, 2015) , (Prabaharan, D. et al, 2016) who also matched data with JCPDS database.

In the other hand, Fig. 2. shows a diffractogram that corresponds to the prepared catalyst $BiFeO_3$. Crystal form is represented by the presence of peaks at $2\theta = 22.209°$, $31.584°$, $38.911°$, $45.258°$, $50.922°$, $56.209°$,and $65.872°$. At the same time, these positions are assigned to (0 1 2), (1 1 0), (2 0 2), (0 2 4), (1 1 6), (3 0 0), and (2 2 0) lattices of $BiFeO_3$, as reported by (Cadenbach, T. et al, 2019) . Similar results were also reported by other researchers like (Wu, S. et al, 2019) , (Kumar, A. et al, 2016) , and (Sifat, A. et al, 2016), that confirm the presence of the desired compound, size and morphology in the evaluated powder .
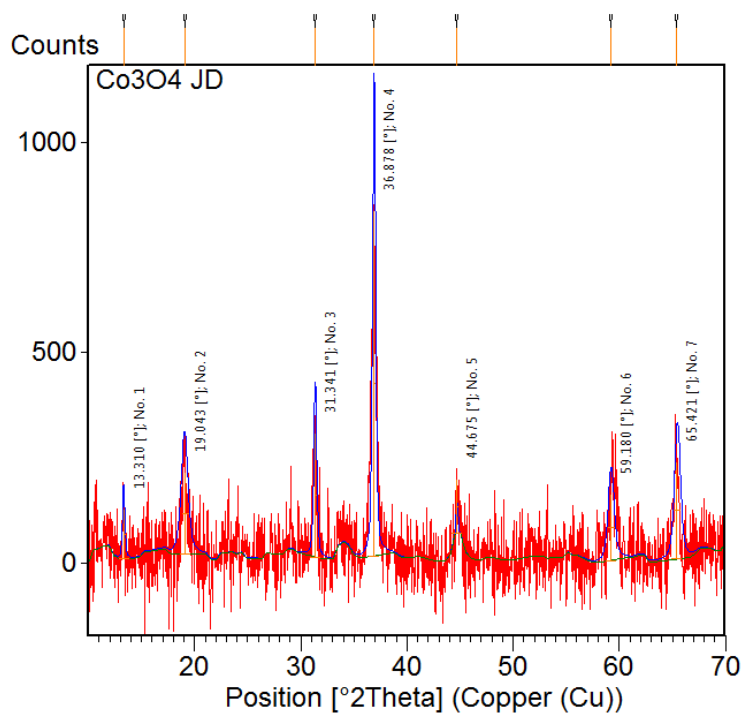
Fig. 1. X-Rays diffractograms of Co_3O_4
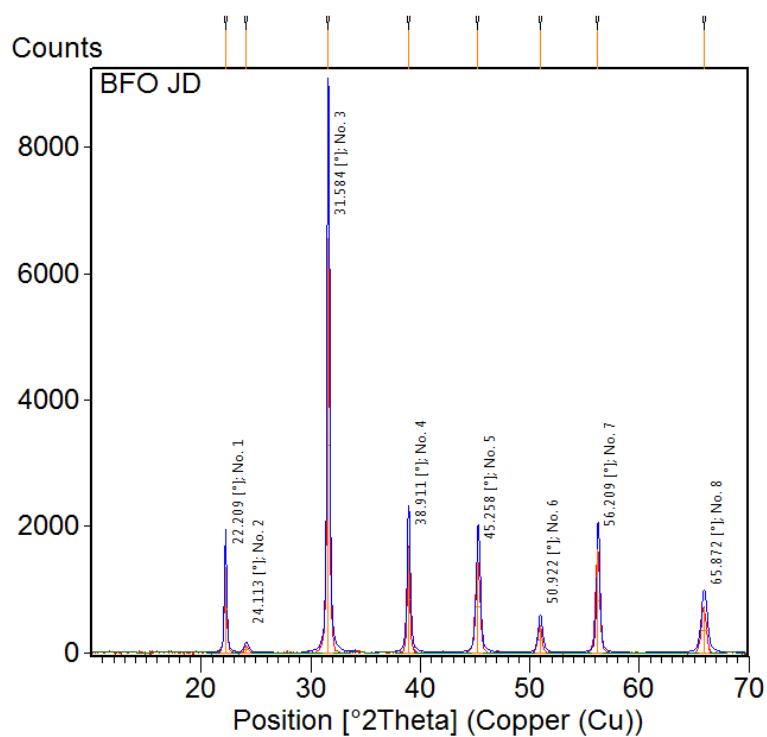

Fig. 2. X-Rays diffractograms of $BiFeO_3$

Fig. 3. shows Transmission electron microscopy images, which indicate well defined nano porous wires of Co_3O_4, that were prepared as described in the previous section by using SBA 15 as hard template. TEM analysis reveals a wire diameter of 9 nm approximately. In addition

Fig. 4. shows TEM images of Co_3O_4 that was synthesize using KIT 6 as hard template. TEM images analysis show particle diameter between 12 nm - 14 nm. These two samples were used as catalyst in a photodegradation process in order to evaluate catalyst activity with different morphologies. Results show that both samples have very similar adsorption capabilities thanks to C_3O_4 great ability to adsorb organic dyes. Therefore, both samples show to perform pretty much in the same range with an small enhanced adsorption capability for Co_3O_4 synthesized with KIT 6 as hard template. In the other hand, Fig. 5. shows TEM images of synthesized $BiFeO_3$ nanowires after leaching degradation of SBA 15 hard template. TEM analysis for this sample reveal a wire diameter of 14 nm.
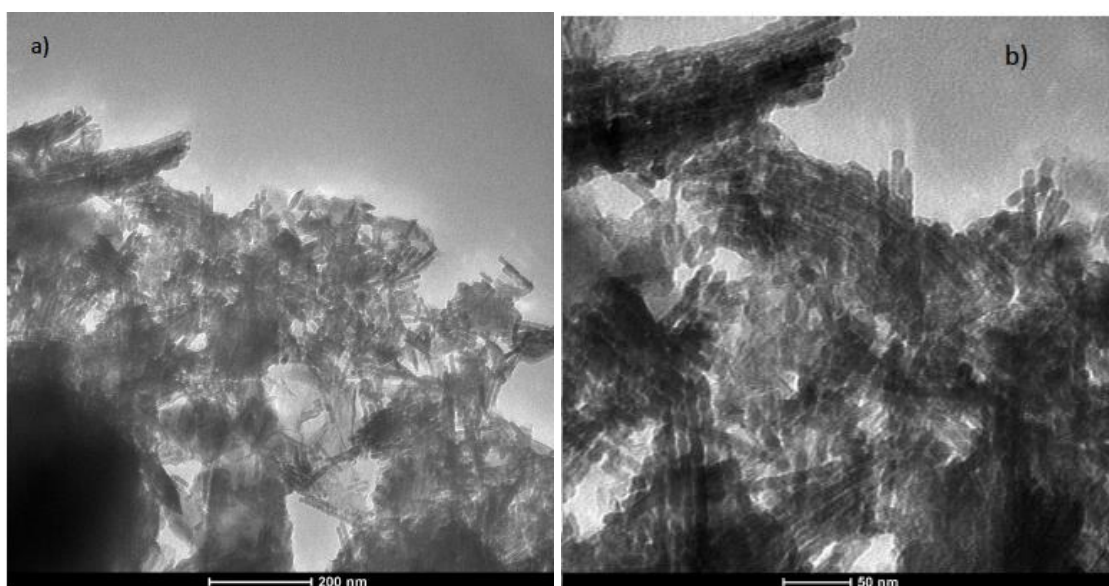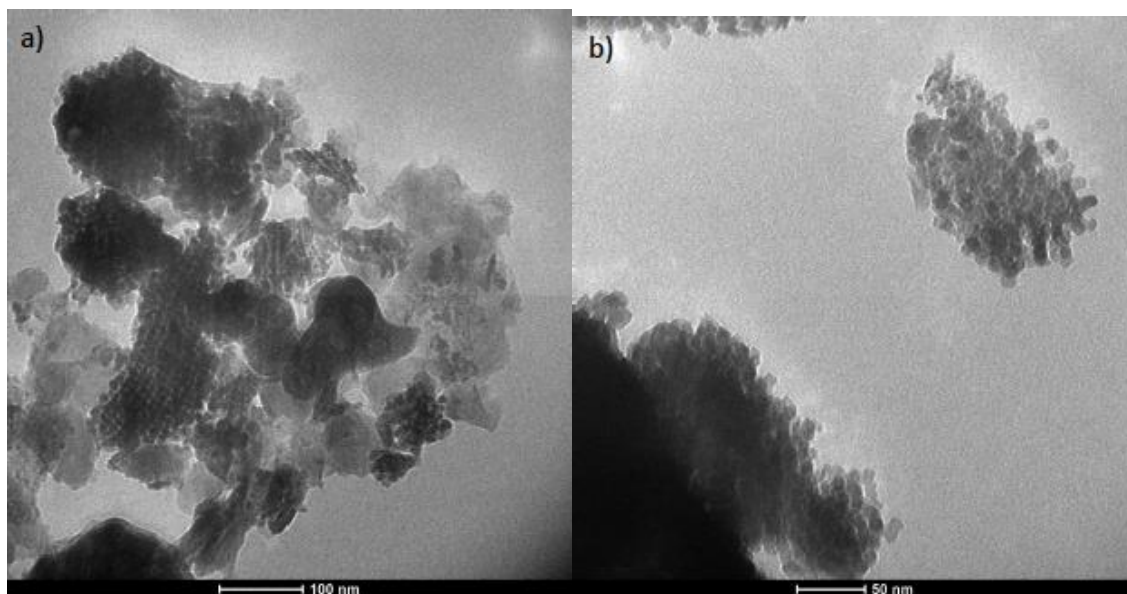

Fig. 3. TEM images of Co_4O_4 samples using SBA 15 as hard template
  a) TEM image of Co_3O_4 nanowires at 200 nm
  b) TEM image of Co_3O_4 nanowires at 50 nm

Fig. 4. TEM images of Co₄O₄ samples using KIT 6 as hard template
c)   *TEM image of Co₃O₄ nanoparticles at 100 nm*
d)   *TEM image of Co₃O₄ nanoparticles at 50 nm*

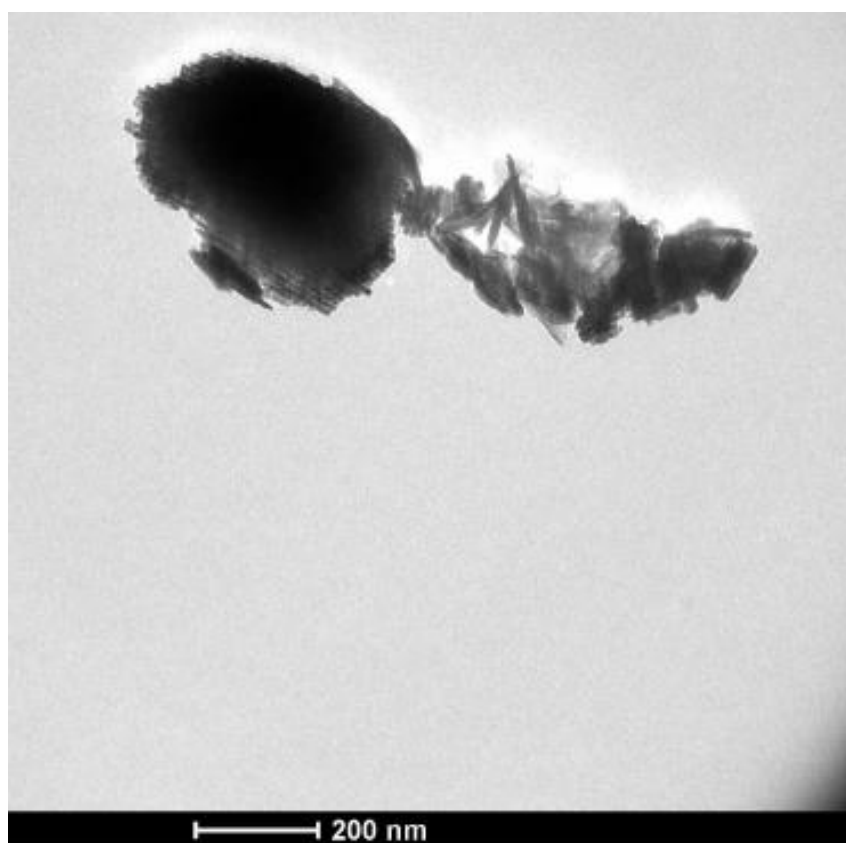*Fig. 5. TEM images of BiFeO₃ nanowires using SBA 15 as hard template*

3.2 Photocatalytic properties of Co₃O₄ and BiFeO₃

Photocatalytic properties of Co_3O_4 and $BiFeO_3$ were evaluated independently, by using a photoreactor with a high LED emission of > 350 nm. Data was recorded from 350 nm to 760 nm wavelength values. In a typical experiment a 50 mg/L solution of Rhodamine B was used to evaluate the photocatalytic capabilities of both compounds. Also 1 hour of darkness under vigorous stirring was allowed in order to reach an adsorption / desorption equilibrium (Cadenbach, T. et al, 2019). After one hour without light, the photoreactor was turned on for photodegradation experiments. Fig. 6. shows a UV-vis spectra of an adsorption experiment using Co_3O_4 as adsorbent. Peak absorbance occurs at 554 nm which it's characteristic of fluorescent dyes (Ahsaine, A. et al, 2014). This experiment was carried out in the absence of light, in order to evaluated this compound's adsorption capability after 5.5 hours. Subsequently processed data produced Fig. 7, which shows plot of C/C0 as function of time of contact with the catalyst. In this relationship C represents the residual concentration after a "t" time and C0 represent the initial concentration of RhB (Devi, L. Aruna, L. 2014). Fig. 6 displays how 50 % of RhB was adsorbed during the first hour of the adsorption process
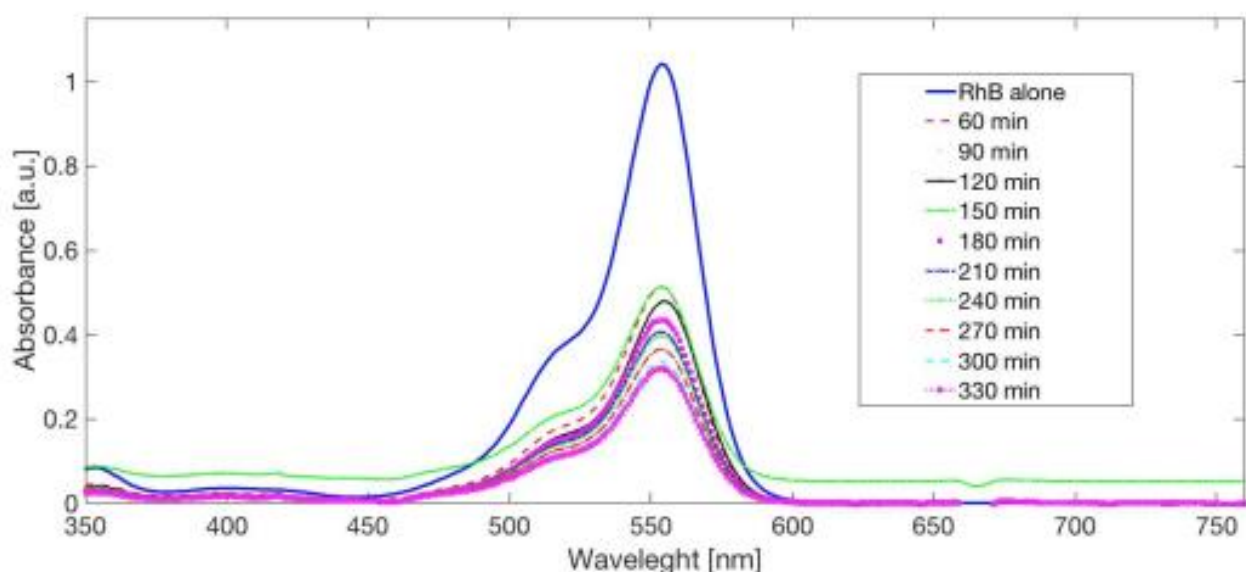

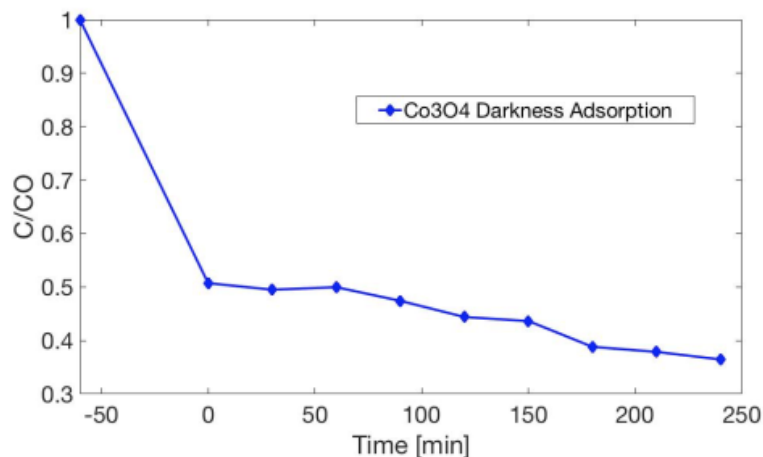*Fig. 6. UV-vis spectra of adsorption experiment with Co₃O₄ in total darkness*

Fig. 7. Adsorption of RhB in the absence of light activation of Co_3O_4

After having satisfactory adsorption results for Co_3O_4, photocatalytic capability was evaluated for the same compound. These results have been displayed in Fig. 8 which compares adsorption in the absence of light with photodegradation of RhB after similar time spams. In this case Fig. 8 plot C and C0 also represent concentration as function of visible light irradiation time. Results show a considerably improvement in the depletion of RhB from a water sample, approximately 80 % of RhB was removed from water after a 4 hour photodegradation period. Adsorption capability was not measured for $BiFeO_3$, because based on the literature, this compound has a better photodegradation capacity (Zhang, N. et al, 2016). Fig. 9, shows a Uv-vis spectra of photodegradation experiments that were carried out under same synthetic conditions as Co_3O_4. A similar solution of 50 mg/L RhB was used. Catalyst was added to 50 mL of RhB sample under vigorous stirring. Absorbance displayed in Fig. 10 show the photodegradation of RhB with $BiFeO_3$ which was measured for 4 hours since the photoreactor was turned on.
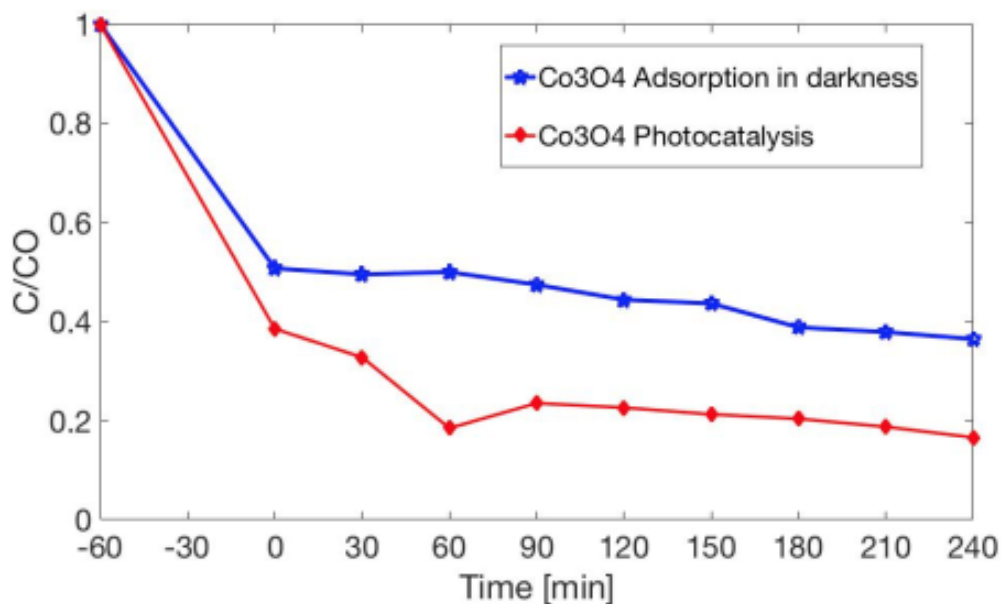
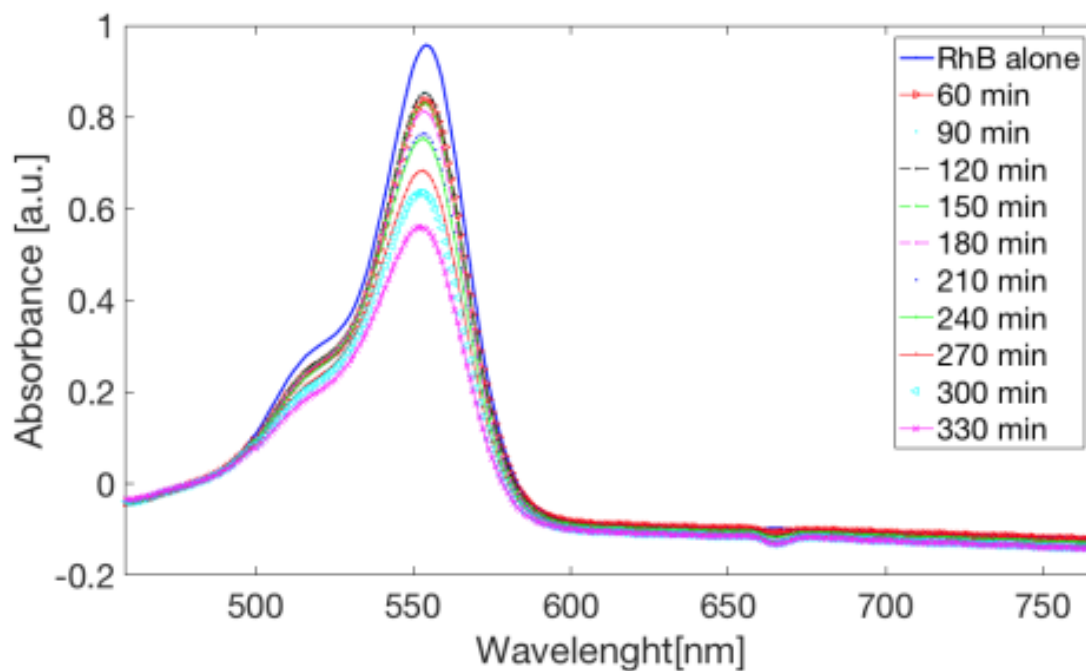*Fig. 8. Co₃O₄ removal of RhB with and without light incidence*

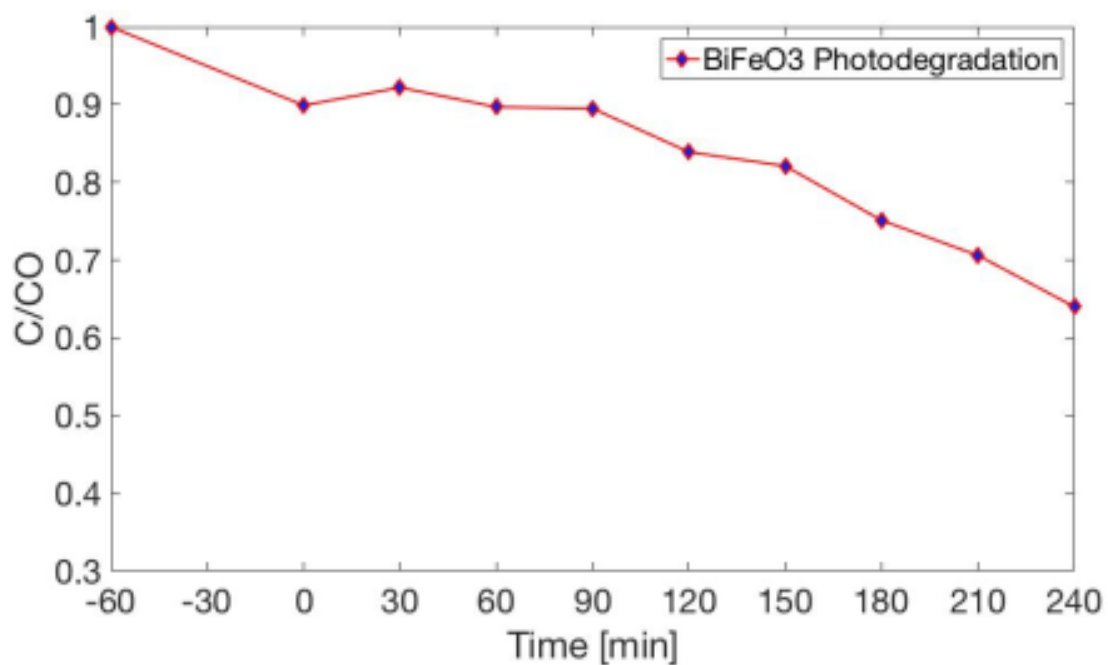*Fig. 9. UV-vis spectra of RhB photodegradation with BiFeO3*

Fig. 10. Photodegradation graphic of RhB using BiFeO₃ as a photocatalyst.
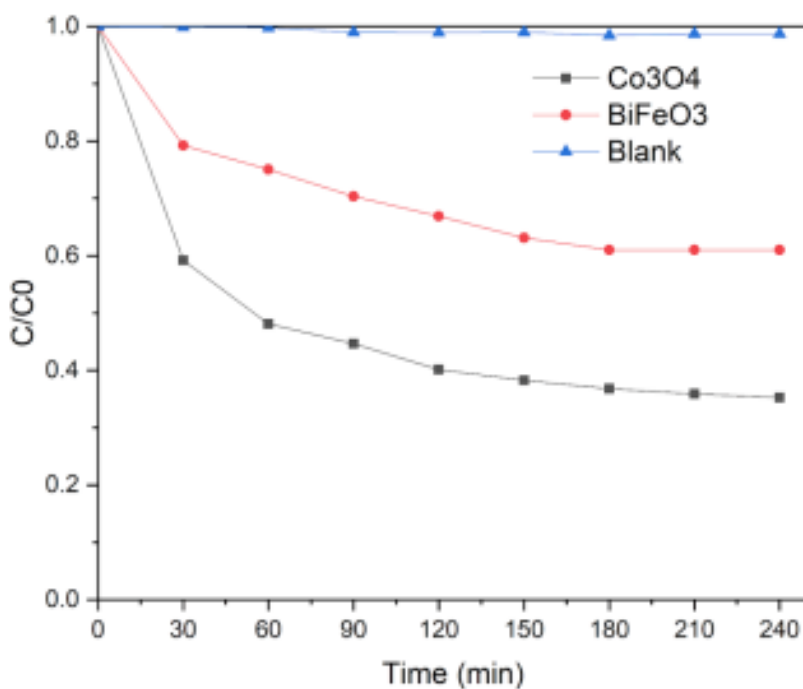

Fig. 11. Photodegradation comparison graphic of RhB using Co₃O₄, and BiFeO₃ as a photocatalysts.

Fig. 11, shows a comparison of RhB photodegradation using both catalysts separately.

These results reveal a better capability of Co_3O_4 to remove RhB from water. Additionally Fig.

11 shows that blank samples didn't show a significant photodegradation, which show a great photo stability as stated in the literature (Raha, S. et al, 2018). .

Subsequently, same experiments were carried out a second time, however two extra chelating agents were added for this group of experiments.

Nitriloacetic Acid (NTAA), and Ethylenediaminetetraacetic acid (EDTA) were chosen for their capability to sequestrate metal ions and form coordination complexes (Pardo, M. 2000), which allowed the formation of a composite material between both catalyst, and improved their degradation capability. Fig. 12 show a comparison between degradation/adsorption capabilities of the catalyst after the addition of chelating agents NTAA, and EDTA.
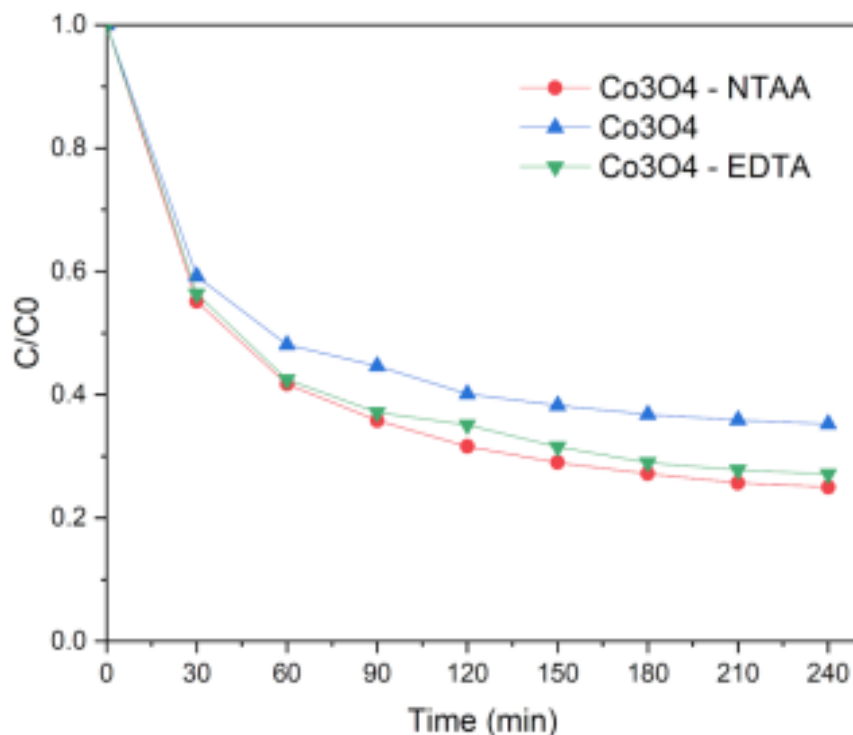

Fig. 12. a) Improved catalyst capacity of Co$_3$O$_4$ with the addition of NTAA /EDTA
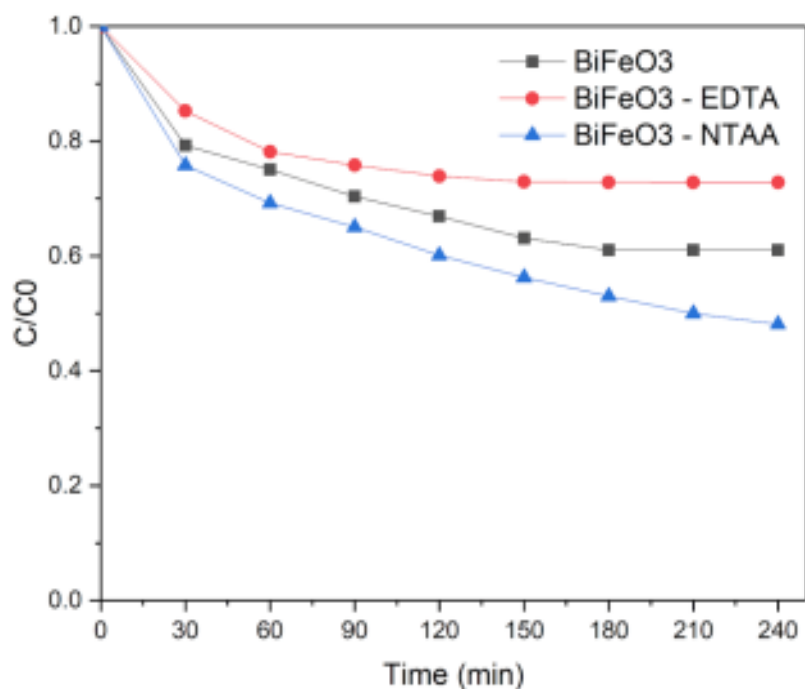
Fig. 12. b) Improved catalyst capacity of BiFeO₃ with the addition of NTAA /EDTA

A composite material was produced by adding the two catalyst straight to the RhB solution, and adding NTAA, and EDTA separately to evaluate RhB removal. Fig. 13 compares degradation of three composite materials that were synthetized in this study, and shows that composite with NTAA has a better degradation / adsorption capacity compared with composited with EDTA, and a composite prepared with nanocasting technique described previously.
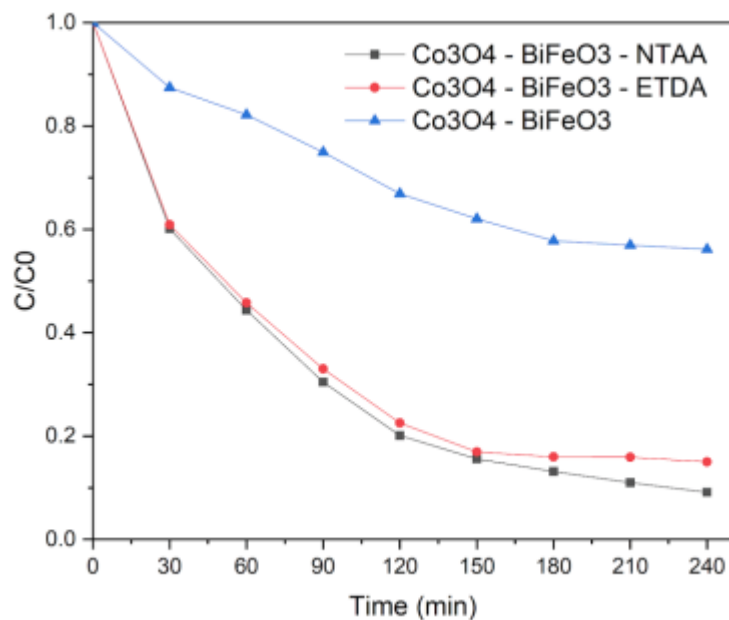
Fig. 13. Degradation / adsorption of RhB with composite materials

To ensure the composite degradation capability, desorption experiments were carried out. Fig. 14 shows a desorption approximately of 90% of RhB from Co_3O_4 plus NTAA, with the addition of a solution containing ethylene glycol, propanol, ethanol, and distilled water. This experiment proves the adsorption capability of Co_3O_4, and the fact that this component by themself does not degraded RhB. In the other hand Fig. 15 shows a desorption experiments of composite materials prepared with chelating agents. Results indicate that after the composite reach almost a 90 % RhB removal in the photodegradation portion, as shown in Fig. 13, when a desorption took place with the recovered catalyst, it only desorbed approximately 6% of RhB, which proves in fact that composite Co_3O_4 / $BiFe_3$ + NTAA removes and degrade RhB in an very efficient way.
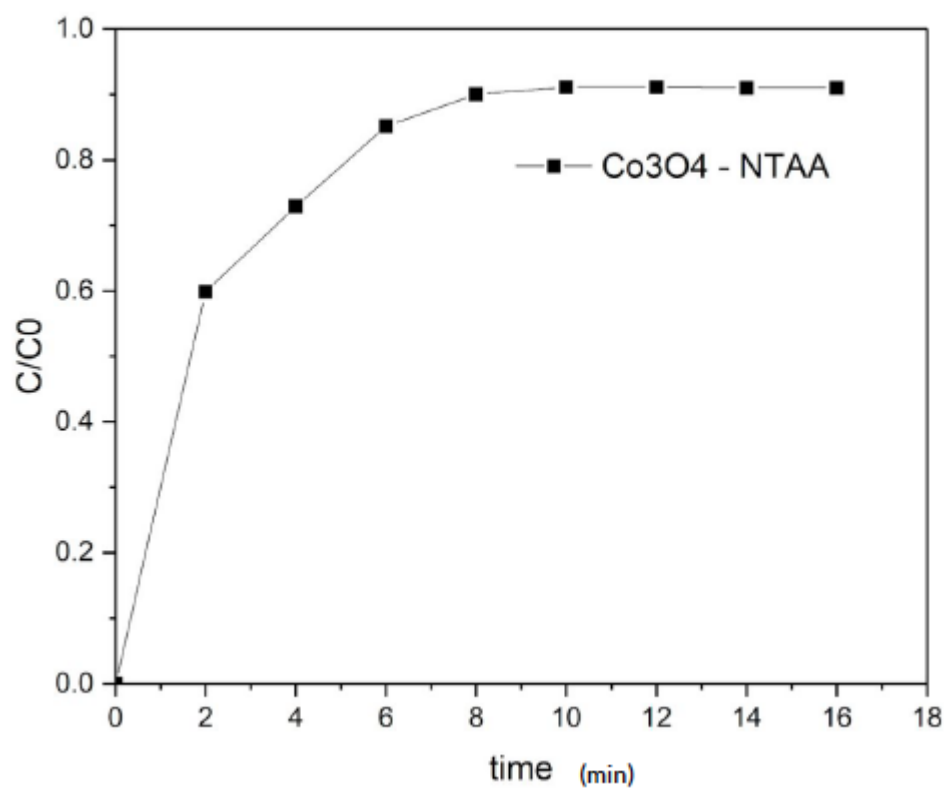
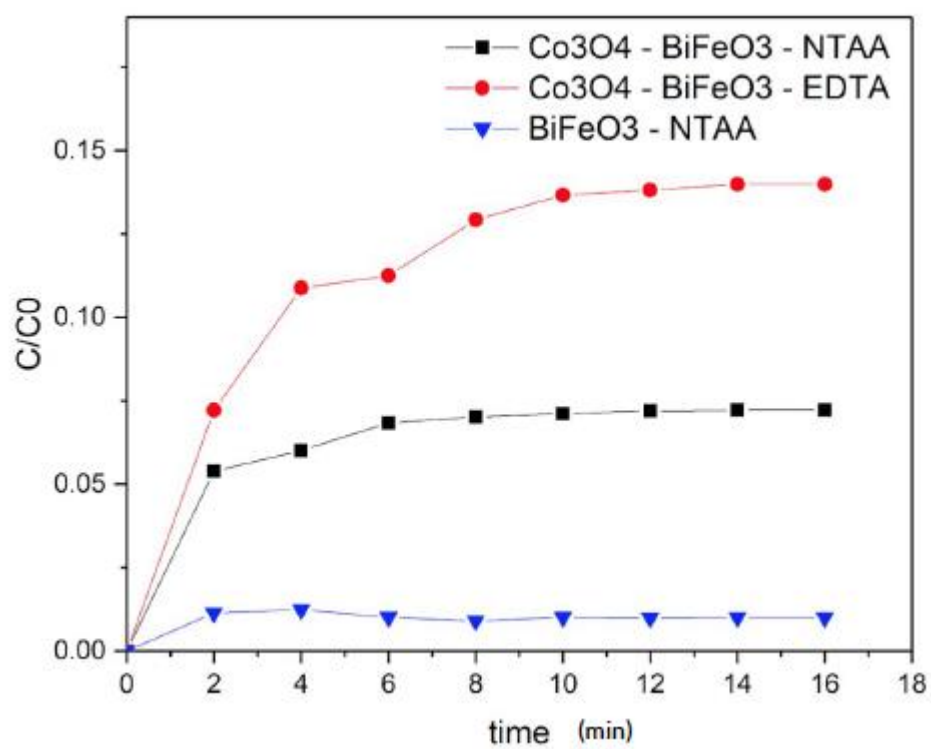*Fig. 14. Desorption experiment of Co$_3$O$_4$ + NTAA*

Fig. 15. Desorption experiment of composite materials

4. Conclusions

Summarizing, a successful synthesis process of mesoporous materials such as SBA 15, KIT 6, and Co_3O_4 was performed, using nanocasting technique. This first two materials serve as hard templates to prepared a highly active $BiFeO_3$ photocatalyst. Characterization shown that the catalyst were in fact Co_3O_4 and $BiFeO_3$ which were added together with the help of two chelating agents NTAA, and EDTA.

A composite material consisting of two semiconductors that have highly enhanced adsorption / degradation properties was synthesized, and its capability to remove RhB as organic dye pollutant was confirmed with desorption experiments that confirm a high rate of degradation of the pollutant from a water sample

5. Acknowledgments

6. References

Ahsaine, A. Hassan & Taoufyq, Aziz & Ezahri, Mohamed & Abdeljalil, Benlhachemi & Bakiz, Bahcine & Villain, Sylvie & Arab, Madjid & Guinneton, F. & Gavarri, Jean-Raymond. (2014). Synthesis, characterization and photocatalytic activity of ZnMO4 system (M= Mo6+, W6+). Journal of Materials and environmental science. 5. 2449-2454.

Binitha, P.V. Suraja, Z. Yaakob, M.R. Resmi, P.P. Silija,(2010) Simple synthesis of Co3O4 nanoflakes using a low temperature sol-gel method suitable for photodegradation of dyes, J. Sol-Gel Sci. Technol. 53 466–469.

Cadenbach, T., Lascano, L., Costa, C., Vizuete, K., & Debut, A. (2019). Size-tunable fabrication of BiFeO3 nanoparticles with enhanced visible-light photocatalytic activity using a facile co-precipitation method. Materials Research Express. doi:10.1088/2053-1591/ab37bc

Chen, X. Si, J. Yu, H. Bai, X. Zhang, (2015) Doping nano-Co2O3 surface with bigger nanosized Ag and its photocatalytic properties for visible light photodegradation of organic dyes, Appl. Surf. Sci. 330 191–199.

Damania, Richard; Desbureaux, Sébastien; Rodella, Aude-Sophie; Russ, Jason; Zaveri, Esha. 2019. Quality Unknown : The Invisible Water Crisis. Washington, DC: World Bank. © World Bank.

Deng, X., Chen, K., & Tüysüz, H. (2016). Protocol for the Nanocasting Method: Preparation of Ordered Mesoporous Metal Oxides. Chemistry of Materials, 29(1), 40–52. doi:10.1021/acs.chemmater.6b02645

Devi, L.Gomathi & M.L., Aruna. (2014). Synergistic effect between orthorhombic α-Sulfur and TiO2 as Co-photocatalysts for efficient degradation of methylene blue: A mechanistic approach. Journal of Molecular Catalysis A: Chemical. 391. 10.1016/j.molcata.2014.04.012.

Edla, R., Patel, N., El Koura, Z., Fernandes, R., Bazzanella, N., & Miotello, A. (2014). Pulsed laser deposition of Co3O4 nanocatalysts for dye degradation and CO oxidation. Applied Surface Science, 302, 105–108. doi:10.1016/j.apsusc.2013.10.174

Grossman, G. M., & Krueger, A. B. (1995). Economic Growth and the Environment. The Quarterly Journal of Economics, 110(2), 353–377. doi:10.2307/2118443

Gao T, Chen Z and Huang Q, (2015) A review: preperation of Bismuth ferrite nanoparticles and its applications in visible-light induced photocatalysis Reviews Advanced Materials Sciences 40 97–109

Hassanpour, M., Safardoust-Hojaghan, H., & Salavati-Niasari, M. (2017). Degradation of methylene blue and Rhodamine B as water pollutants via green synthesized Co 3 O 4 /ZnO nanocomposite. Journal of Molecular Liquids, 229, 293–299. doi:10.1016/j.molliq.2016.12.090

Hodges, B. C., Cates, E. L., & Kim, J.-H. (2018). Challenges and prospects of advanced oxidation water treatment processes using catalytic nanomaterials. Nature Nanotechnology, 13(8), 642–650. doi:10.1038/s41565-018-0216-x

National Council of Textile Organizations NCTO. (2017). 2018 State of the U.S. textile industry address delivered by NCTO chairman bill mccrary.

Pardo, M. T. (2000). Sorption of lead, copper, zinc, and cadmium by soils: effect of nitriloacetic acid on metal retention. Communications in Soil Science and Plant Analysis, 31(1-2), 31–40. doi:10.1080/00103620009370418

Prabaharan, D. D. M., Sadaiyandi, K., Mahendran, M., & Sagadevan, S. (2017). Precipitation method and characterization of cobalt oxide nanoparticles. Applied Physics A, 123(4). doi:10.1007/s00339-017-0786-8

Pereira, L. and Alves, M.(2014) Dyes—Environmental Impact and Remediation 2014 (Dordrecht: Springer) p 201422

Sharifzade, G., Asghari, A., & Rajabi, M. (2017). Highly effective adsorption of xanthene dyes (rhodamine B and erythrosine B) from aqueous solutions onto lemon citrus peel active carbon: characterization, resolving analysis, optimization and mechanistic studies. RSC Advances, 7(9), 5362–5371. doi:10.1039/c6ra23157h

Saeed, M., Muneer, M., Mumtaz, N., Siddique, M., Akram, N., & Hamayun, M. (2018). Ag-Co 3 O 4 : Synthesis, characterization and evaluation of its photo-catalytic activity towards degradation of rhodamine B dye in aqueous medium. Chinese Journal of Chemical Engineering, 26(6), 1264–1269. doi:10.1016/j.cjche.2018.02.024

Sifat, A. A., Aabrar, K. A., Bashar, M. K., Ahmmad, B., Basith, M. A., & Khan, M. Z. R. (2016). Temperature dependent structural studies and magnetic characterization of pure BiFeO3 nanoparticles synthesized by sol-gel method. 2016 9th International Conference on Electrical and Computer Engineering (ICECE). doi:10.1109/icece.2016.7853887

Lam S-M, Sin J-C and Mohamed A R A (2017). Newly emerging visible light-responsive BiFeO3 perovskite for photocatalytic applications: a mini review 2017 Mater. Res. Bull. 90 15–30

Mashayekhi, M. & Ghani, Kamal & Razavi, Reza & shokrolahi, arash & Kiomarsipour, Narges. (2015). Development of Spacecraft Black Thermal Control Coatings Using the Synthesized Mesoporous Co3O4 Pigment. Progress in Color, Colorants and Coating.

Wu, S., Zhang, J., Liu, X., Lv, S., Gao, R., Cai, W., … Fu, C. (2019). Micro-Area Ferroelectric , Piezoelectric and Conductive Properties of Single BiFeO 3 Nanowire by Scanning Probe Microscopy. https://doi.org/10.3390/nano9020190

Kumar, Arun & Pandey, Dhananjai. (2016). The Ground state of BiFeO3: Low temperature magnetic phase transitions revisited.

Raha, s., Ivanov, i., Quazi, n., & Bhattacharya, S. (2008). Photo-stability of rhodamine-B/montmorillonite nanopigments in polypropylene matrix. Applied Clay Science. doi:10.1016/j.clay.2008.06.008

Zhang N, Chen D, Niu F, Wang S, Qin L and Huang Y (2016) Enhanced visible light photocatalytic activity of Gd-doped BiFeO3 nanoparticles and mechanism insight Sci. Rep. 6 26467
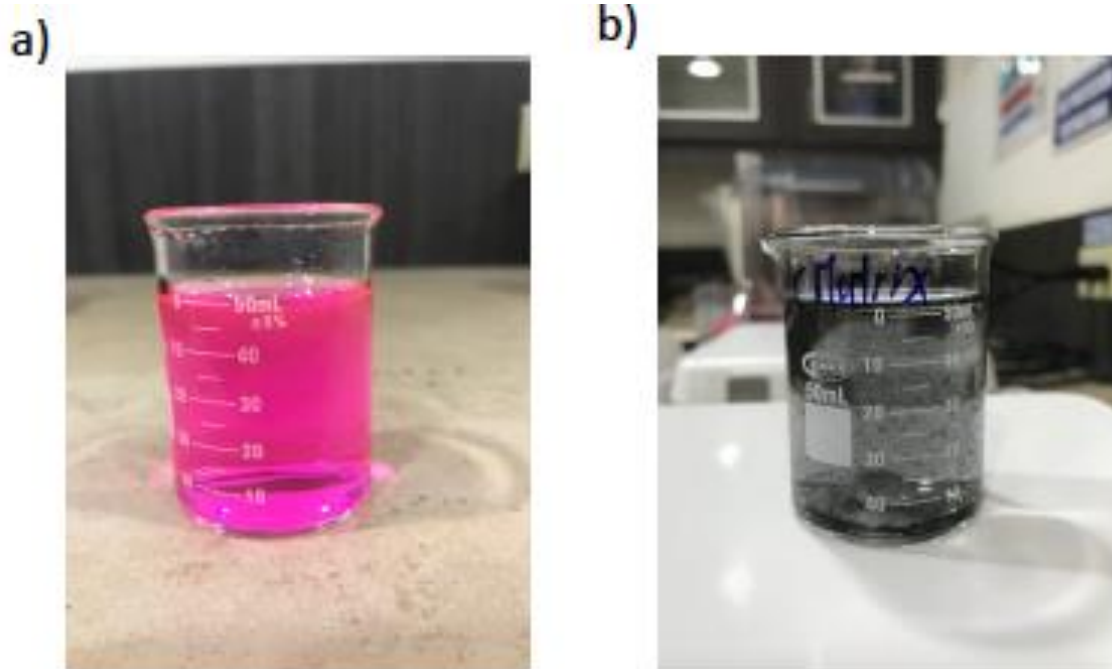
7. Annexes

Fig. 16. Rhodamine B-5 mg/L (left), After adding 50 mg
adsorbent (right)

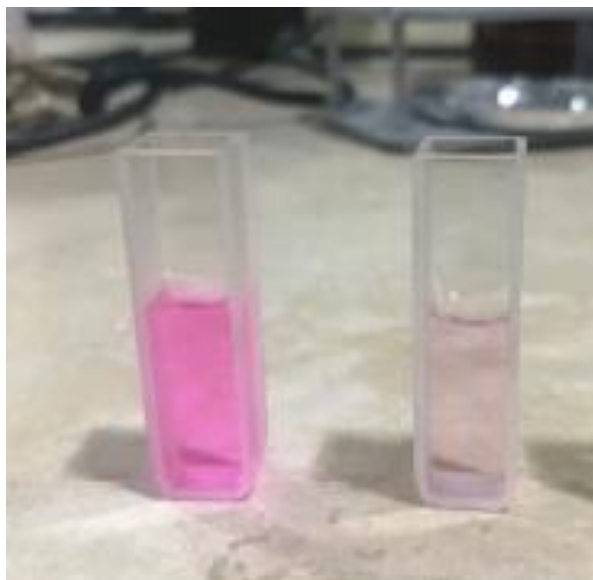*Fig. 17. Photoreactor used in the photodegradation reactions*

Fig. 18. Rhodamine B before and after photodegradation with composite material